Diagn Interv Radiol 2016; 22:224–230

CHEST IMAGING
ORIGINAL ARTICLE

Percutaneous transthoracic localization of pulmonary nodules under C-arm cone-beam CT virtual navigation guidance

Tae Ho Kim
Chang Min Park
Sang Min Lee
H. Page McAdams
Young Tae Kim
Jin Mo Goo

PURPOSE
We aimed to describe our initial experience with percutaneous transthoracic localization (PTL) of pulmonary nodules using a C-arm cone-beam CT (CBCT) virtual navigation guidance system.

METHODS
From February 2013 to March 2014, 79 consecutive patients (mean age, 61±10 years) with 81 solid or ground-glass nodules (mean size, 12.36±7.21 mm; range, 4.8–25 mm) underwent PTLs prior to video-assisted thoracoscopic surgery (VATS) excision under CBCT virtual navigation guidance using lipiodol (mean volume, 0.18±0.04 mL). Their procedural details, radiation dose, and complication rates were described.

RESULTS
All 81 target nodules were successfully localized within 10 mm (mean distance, 2.54±3.24 mm) from the lipiodol markings. Mean number of CT acquisitions was 3.2±0.7, total procedure time was 14.6±5.14 min, and estimated radiation exposure during the localization was 5.21±2.51 mSv. Postprocedural complications occurred in 14 cases (17.3%); complications were minimal pneumothorax (n=10, 12.3%), parenchymal hemorrhage (n=3, 3.7%), and a small amount of hemoptysis (n=1, 1.2%). All target nodules were completely resected; pathologic diagnosis included invasive adenocarcinoma (n=53), adenocarcinoma-in-situ (n=10), atypical adenomatous hyperplasia (n=4), metastasis (n=7), and benign lesions (n=7).

CONCLUSION
PTL procedures can be performed safely and accurately under the guidance of a CBCT virtual navigation system.

With the widespread utilization of low-dose computed tomography (CT) screening, detection of early lung cancers, which manifest as small solid nodules or ground-glass nodules (GGNs), has been possible. According to one large observational cohort study (1, 2), solitary noncalcified pulmonary nodules were detected at the rate of 15%–20% among the high-risk population screened on baseline screening CT and 15% of these nodules proved to be malignant (1, 2). Therefore, it is crucial to safely and accurately diagnose these suspicious nodules that have a high probability of malignancy.

Bronchoscopic biopsy or percutaneous transthoracic needle biopsy (PTNB) using CT have been commonly used for tissue sampling and pathologic confirmation. However, these methods sometimes show limitations for tissue sampling of small or faint lesions. Furthermore, their ability to distinguish between pulmonary adenocarcinomas and their preinvasive lesions has been questioned (3, 4). In this context, video-assisted thoracoscopic surgery (VATS) excision has been utilized in clinical practice. Although VATS excision can be more invasive than PTNB or bronchoscopic biopsy, it can certainly offer a definitive diagnosis for suspicious pulmonary nodules even if they are small or faint (5, 6). VATS excision also provides simultaneous treatment and diagnosis. However, resection of these targets through VATS can be very challenging, and complete resection of the targets sometimes proves impossible, especially when the target nodules are too small or faint for surgeons to detect (7). Therefore, prior to VATS excision for small or faint lung nodules, percutaneous transthoracic localization (PTL) has been commonly performed under imaging guidance using several marking devices or materials (8–10).

Recently C-arm cone-beam CT (CBCT) and state-of-the-art CBCT virtual navigation systems have been introduced in the field of radiologic intervention (11–15). In particular, CBCT virtual navigation systems provide a virtual needle pathway as the needle approaches the target point

From the Department of Radiology (T.H.K., C.M.P. ✉ *cmpark.morphius@gmail.com* S.M.L., J.M.G.), Seoul National University College of Medicine, and Institute of Radiation Medicine, Seoul National University Medical Research Center, Seoul, Korea; the Cancer Research Institute (C.M.P., J.M.G.), Seoul National University, Seoul, Korea; the Department of Radiology (C.M.P., H.P.M.), Duke University Medical Center, Durham, NC, USA; the Department of Thoracic Surgery (Y.T.K.), Seoul National University College of Medicine, Seoul, Korea.

Received 14 July 2015; revision requested 30 July 2015; last revision received 21 September 2015; accepted 22 September 2015.

Published online 22 March 2016.
DOI 10.5152/dir.2015.15297

and additional navigation after the skin entry site and the target point within the body are located using preprocedural CBCT data (11). This brand-new guiding system has the technical advantage of additional safety features, including accurate and flexible needle route selection based on three-dimensional (3D) volume CT data, real-time fluoroscopic navigation, and comfortable operating conditions through an open gantry system (11). Due to its inherent advantages and virtual navigation systems, CBCT has great potential to provide very accurate and safe localization of small or faint pulmonary nodules. To the best of our knowledge, there have been no studies dealing with CBCT virtual navigation-guided PTL of pulmonary nodules to date. Thus, the purpose of our study was to describe our initial experiences with PTL of pulmonary nodules using a CBCT virtual navigation guidance system.

Methods

The Institutional Review Board of Seoul National University Hospital approved this retrospective study with a waiver of the requirement for patients' informed consent for inclusion into this study. Written informed consent for PTL under the guidance of a CBCT virtual navigation system was obtained from each patient after explanation of all potential risks and benefits.

Patients and nodules characteristics

From February 2013 to March 2014, 81 consecutive PTLs for 81 pulmonary nodules (mean size, 12.36±7.21 mm; range, 4.8–25mm) in 79 consecutive patients (37 males and 42 females; mean age, 61±10 years; range, 39–80 years) were included in this study. There were seven solid nodules, 48 pure GGNs, and 26 part-solid GGNs. Most of these pulmonary nodules (91.4%) presented ground glass opacity and because these characteristics have high risk of malignancy, the surgeons requested lipiodol localization before VATS excision. The remaining seven solid nodules were requested to have lipiodol localization, because they showed relatively small size (mean size, 7.7±1.86 mm) with suggestive findings of malignancy. The mean distance from nodule to the pleura was 24.9±13 mm (range, 0.4–66 mm). Nodules were detected on screening CTs in 53 patients, during diagnostic work-ups for underlying malignancies in 23 patients, and were detected for symptom evaluation of blood-tingled sputum in three. There were 52 never-smokers, 22 ex-smokers, and five current smokers. The average smoking amount was 21.5 pack-years (range, 4–75 pack-years). Characteristics of the patients and nodules are summarized in Table 1.

Procedural details of CBCT virtual navigation-guided PTLs

All PTL procedures were performed under the guidance of CBCT virtual navigation system in combination with CBCT system (AlluraXperFD20; Phillips Healthcare) and virtual guiding software (XperCT and XperGuide software; Phillips Healthcare) by, or under the supervision of, a chest radiologist (C.M.P. with 10 years of experience in image-guided thoracic intervention). All PTL procedures were performed on the same day or one day prior to VATS in collaboration with the thoracic surgery team. The procedural details are as follows:

1. Prior to the PTL procedure, the target nodule was carefully reviewed on the diagnostic CT previously taken and the optimal and safest trajectory was decided by the operators.

2. For PTL procedures, each patient was positioned on a CBCT table in either a supine or prone position depending on the location of lung nodule (Fig. 1a). After properly positioning the patient, preprocedural CBCT was performed in the region of interest during a single breath-hold in inspiration or expiration, as appropriate. Simultaneously, C-arm rotated 240˚ in 5.2 seconds

Table 1. Nodule characteristics

Characteristics	Values
Nodule size (mm), mean±SD	12.36±7.21 (range; 4.8–25)
Distance from nodule to pleura (mm), mean±SD	24.90±13 (range; 0.4–66)
Nodule feature (n)	
Solid nodule	7
Pure GGN	48
Part-solid GGN	26
Location (n)	
Right upper lobe	23
Right middle lobe	3
Right lower lobe	26
Left upper lobe	16
Left lower lobe	13

SD, standard deviation; GGN, ground-glass nodule; n, number of patients.

Main points

- C-arm cone-beam CT (CBCT) virtual navigation systems based on three-dimensional CBCT data could guide percutaneous transthoracic localization for the small lung nodule very accurately.
- Virtual navigation guidance enables safe localization procedures for small lung nodules prior to video-assisted thoracoscopic sugery (VATS).
- Nodule localization with lipiodol can be performed safely and precisely using CBCT.

Figure 1. a, b. Patients were placed in supine or prone position according to the proper needle trajectory established based on the prior diagnostic CT **(a)**. After local anesthesia, a 21-gauge needle was introduced to the target nodule under the guidance of fluoroscopy **(b)**.

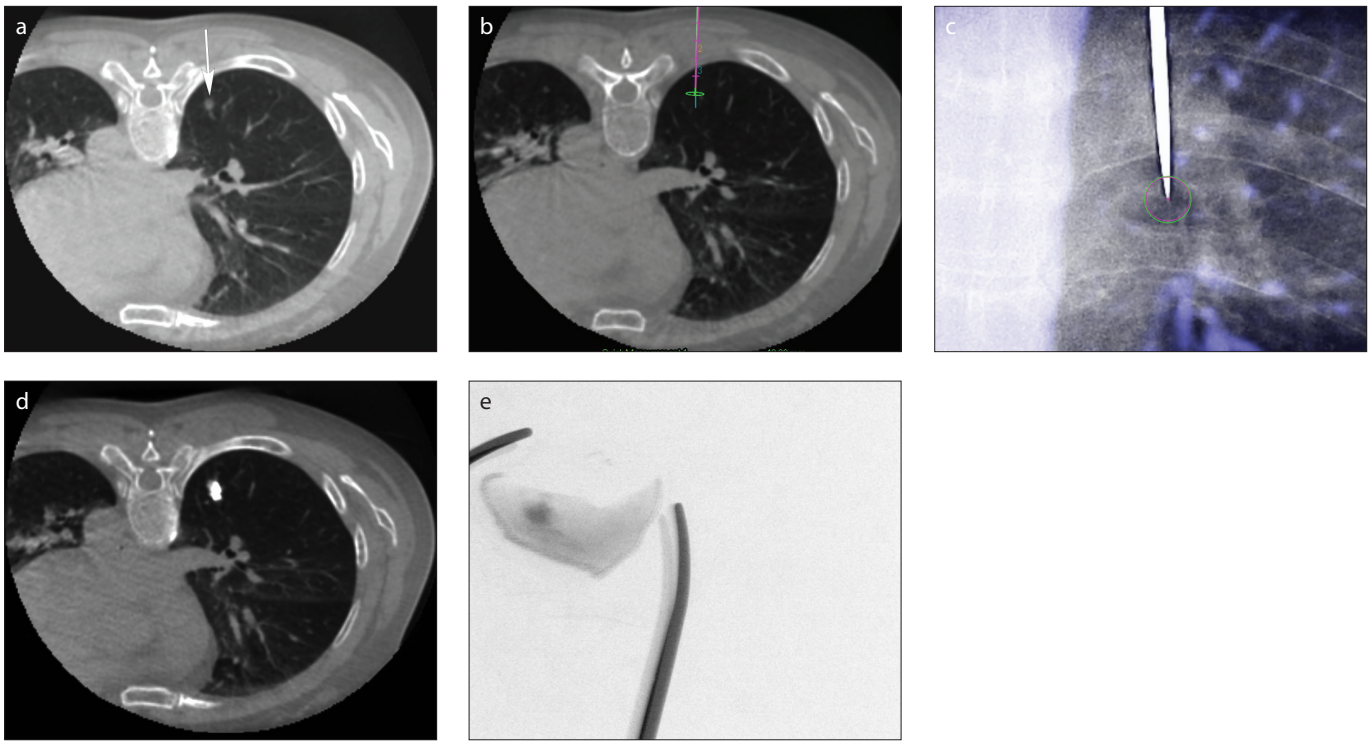

Figures 2. a–e. A 63-year-old female who underwent a lower anterior resection due to colon cancer, followed by cone-beam CT (CBCT)-guided percutaneous transthoracic localization (PTL) for a 6 mm pure ground-glass nodule (GGN) in the right lower lobe of the lung. This nodule, undetectable by fluoroscopy, can be easily visualized through preprocedural CBCT **(a)**. Proper skin entry site and target point of lipiodol marker placement were carefully planned using 3D CBCT data with virtual navigation guidance software **(b)**. The CBCT virtual navigation system enables the automatic alignment of X-ray tube, target point and detector, providing "bull's eye view," then the needle was carefully introduced to the intended localization site under fluoroscopic guidance **(c)**. Afterwards, lipiodol was slowly and carefully injected, with no procedure-related complications **(d)**. Localized marker was easily detectable with intraoperative fluoroscopy before the excision of the target nodule and the lipiodol marker **(e)**. This nodule was identified as adenocarcinoma-in-situ.

generating 312 images in a 512×512 matrix (Fig. 2a).

3. After the preprocedural CBCT was performed, the projectional images acquired were automatically transmitted to a commercially-available dedicated workstation (Xtravision; Philips Healthcare) and 3D CT images were reconstructed using 1 mm thick multiplanar reformations in axial, coronal, and sagittal planes with a total reconstruction time of 25 seconds. Subsequently, operators determined the proper skin entry site, target points of localization-marker placement, and trajectories with distance to target points using the virtual navigation software (XperGuide) (Fig. 2b). Target points of localization were determined within a 10 mm range around target lung nodules.

4. According to the needle trajectories determined using the virtual guidance software, C-arm gantry of the CBCT system automatically rotated until the skin (red circle) and target points (green circle) were superimposed making a "bull's eye view" and the virtual navigation system virtually marked the skin entry site on fluoroscopy (Fig. 2c). After local anesthesia at the point of entry with 2% lidocaine, a 21-gauge needle was carefully introduced to the intended localization site through the planned skin-entry site under fluoroscopic guidance, keeping the needle angle in the "bull's eye view" (Fig. 1b). After the needle was placed in the planned target point, intraprocedural CBCT was performed to check the exact location of the needle tip around the targeted pulmonary nodule. If the needle tip was located exactly at the target point, the inner stylet of the needle was withdrawn and lipiodol (Guerbet Laboratories) was slowly and carefully injected through the needle under surveillance via fluoroscopy. Maximum capacity of lipiodol was predefined as 0.2 mL (mean amount, 0.18±0.04 mL; range, 0.15–0.20 mL) considering the size of radiopaque markers of 1 cm and potential risk of lipiodol embolism (16). Also during lipiodol injection, we carefully monitored the movement of lipiodol droplets using fluoroscopy.

5. Afterwards, postprocedural CBCT was performed to identify the exact location of the lipiodol marker with respect to the target pulmonary nodules (Fig. 2d). Postprocedural complications were also carefully investigated with CBCT images. Blood pressure, heart rate, breathing rate, and the arterial oxygen saturation of all patients were closely monitored throughout the entire procedure.

Data analysis

One radiologist identified the procedural records that included technical success or failure, diameter of lipiodol marker, distance from nodule to lipiodol marker, number of CT exams, total procedure time, radiation exposure through the PTL procedure, procedure-related complications, and the time interval between the PTL procedure and the VATS. Total procedural time was defined as the time period from the administration of local anesthesia to the end of postprocedure CBCT. Technical success was defined as the location of the lipiodol markers within a 10 mm range around target nodules on postprocedural CBCT images. Radiation exposure was also recorded during the entire PTL procedures (both the fluoroscopy dose and the CBCT dose) and total dose area product (DAP) during the

fluoroscopy and the CBCT acquisition was recorded for the absorbed radiation doses (mGy). Subsequently, DAPs were converted into effective doses using the conversion factor of 0.45 mSv/Gy·cm^2 obtained from our previous study (11).

Surgical findings, such as the visibility of the radiopaque lipiodol marker under intraoperative C-arm fluoroscopy and success in surgical resection of both the marker and the target nodule, were recorded (Fig. 2e). In addition, all pathologic reports of VATS specimens were reviewed to evaluate the final diagnosis of targeted lung nodules. All lesions were evaluated in terms of the pathologic diagnosis of the target nodule.

Results

The technical success rate of PTLs under CBCT virtual navigation guidance was 100% (81/81). The mean diameter of lipiodol markers was 9.75±9.09 mm (range, 5–19 mm) and the distance from target nodules to lipiodol markers was 2.54±3.24 mm (range, 0–10 mm). Mean overall DAP during the total procedure was 11730±5463.6 mGy cm^2. Thus, the mean effective dose during CBCT virtual navigation-guided PTLs was 5.21±2.51 mSv in the present study. The procedural records and radiation doses of the 81 cases are summarized in Table 2. Postprocedural complications occurred in 14 cases (17.3%). Small pneumothorax occurred in 10 cases (12.3%), parenchymal hemorrhage in three cases (3.7%), and a small amount of hemoptysis occurred in one case (1.2%). However, there were no serious complications that required any further procedures such as chest drainage catheter insertion or embolism events.

VATS excision was performed on the same day in 68 patients (84%) and the next day in 13 patients (16%) after PTLs. Lipiodol markers were identifiable in all cases under intraoperative fluoroscopy (n=81) and all radiopaque lipiodol and targeted nodules were successfully resected with a negative surgical margin through VATS. Pathologically, all nodules were definitively diagnosed. Diagnoses of the 81 nodules included invasive adenocarcinoma (n=53), adenocarcinoma-in-situ (n=10), metastasis (n=7), atypical adenomatous hyperplasia (n=4), and nonspecific benign pathologies (n=7) (Table 3).

Table 2. Procedural details of CBCT virtual navigation-guided PTLs

Characteristics	Values
Technical success rate, n/N (%)	81/81 (100)
Amount of lipiodol (mL), mean±SD	0.18±0.04 (range; 0.15–0.2)
Diameter of lipiodol (mm), mean±SD	9.75±9.09 (range; 5–19)
Distance from nodule to marking (mm), mean±SD	2.54±3.24 (range; 0–10)
Patient's position, n	
Supine	22
Prone	59
Number of CBCT data acquisitions, mean±SD	3.2±0.7 (3–7)
Total procedure time (min), mean±SD	14.6±5.14 (range; 9–31)
Effective radiation dose (mSv), mean±SD	5.21±2.51 (range; 0.67–13.09)
Postprocedural complications, n (%)	
Small pneumothorax	10 (12.3)
Parenchymal hemorrhage	3 (3.7)
Small hemoptysis	1 (1.2)
Time interval between PTL and operation, n (%)	
Same day	68 (84)
Next day	13 (16)

CBCT, C-arm cone-beam computed tomography; PTL, percutaneous transthoracic localization; n, number of patients; SD, standard deviation.

Table 3. Pathologic diagnosis of nodules

Pathologic diagnosis	Number of nodules
Invasive adenocarcinoma	53
Adenocarcinoma-in-situ	10
Metastatic nodule	7
Atypical adenomatous hyperplasia	4
Benign nodules	7
Smooth muscular proliferation	1
Nonspecific inflammation	2
Reactive hyperplasia	1
Fibrotic nodule	2
Anthracofibrotic lesion	1

Discussion

In this study, we found that all 81 PTL procedures under CBCT virtual navigation guidance were successful, delivering lipiodol markers within 10 mm distance from the targeted pulmonary nodules before VATS excision. Postprocedural complications were relatively low and total procedure time was short. These targeted nodules were successfully resected with a negative surgical margin through VATS.

VATS excision has several benefits, including shorter hospitalizations, less pain for patients, lower postoperative wound problems, and the preservation of normal lung parenchyma compared with conventional thoracic surgery. In general, the sensitivity and specificity of malignancy through VATS excision is known to be 100% (5, 6). However, VATS excision can sometimes be very challenging, especially when the pulmonary nodules are too small, too faint, or too deeply located for surgeons to detect through palpation (7). In particular, pure or part-solid GGNs on CT, which represent adenocarcinoma containing lepidic components (or its preinvasive lesions), could be typical examples of this kind of challenge, even though these nodules are located just

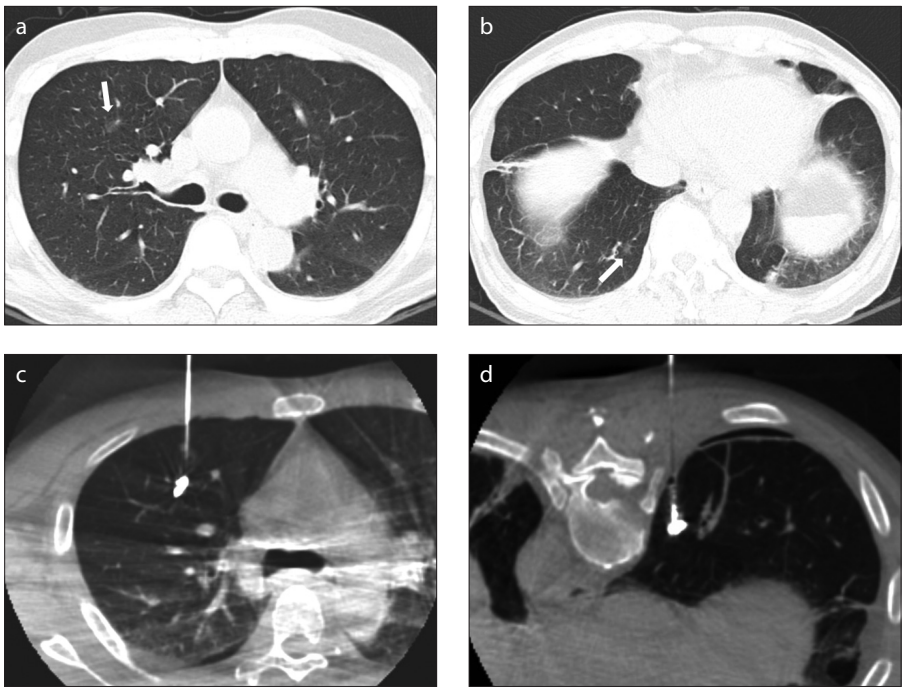

Figures 3. a–d. A 70-year-old male who had CBCT-guided PTL for two different GGNs. Chest CT for lung cancer screening shows an 8 mm pure GGN in the right upper lobe of the lung **(a)** and a 6 mm pure GGN in the right lower lobe of the lung **(b)**. Panels **(c)** and **(d)** show the localization of GGNs under CBCT with virtual navigation guidance. Patient was placed in supine position for localization of the GGN in the right upper lobe **(c)**. Then, patient's position was changed to prone for localization of the GGN in the right lower lobe **(d)**. GGN in the right upper lobe was identified as adenocarcinoma-in-situ, while the one in the right lower lobe was identified as atypical adenomatous hyperplasia.

beneath the pleura (17). Therefore, it is essential to perform PTL before VATS excision to guarantee the successful and effective resection of these faint or small, but clinically relevant lesions. Furthermore, operating time has been reported to significantly decrease with PTL compared with patients not undergoing PTL (18).

Several previous studies reported the effectiveness of CT- or CT fluoroscopy (CTF)-guided PTL on small pulmonary nodules (10, 19). However, CT- or CTF-guided PTLs have several inherent disadvantages, such as small and deeply located closed gantry systems, limited real-time guidance, or limited imaging plane orientation of the needle trajectory, which has the potential to deteriorate the operators' performance or confidence (20–23).

Recently, CBCT and CBCT virtual navigation systems have been increasingly used in various fields of radiologic interventional procedures (24–26). CBCT-guided, or CBCT virtual navigation-guided PTNB have been reported to provide very excellent and, at least, equivalent diagnostic accuracy to state-of-the-art CTF-guided PTNB (11, 12, 27). In fact, given the flexible tilting and open gantry system of CBCT, as well as improved guidance of needle trajectory based on 3D volume CT data, operators can perform interventional procedures more comfortably and confidently (Fig. 3). Also we believe that these kinds of technical advantages could be implemented even in localization of small lung nodules, which could lead to lower postprocedural complication rates, providing improved awareness and avoidance of dangerous organs or vessels (Fig. 4).

In our study, technical success rate of PTL procedures was 100%. Technical success of PTL meant that the lipiodol markers were placed within 10 mm from target nodules. The needle did not have to be exactly placed in the target nodule. So, the results of technical success of PTL may not be directly applied to other CBCT-guided procedures such as biopsy, where the needle should hit the nodule precisely.

Postprocedural complications occurred in 14 cases (17.3%) in our study. Small pneumothorax occurred in 10 cases (12.3%), parenchymal hemorrhage in three cases (3.7%), and a small amount of hemoptysis in one case (1.2%). Moreover, there were no serious complications requiring any further procedures such as surgical intervention or needle aspiration. Considering that in CT- or CTF-guided biopsy, postprocedural pneumothorax has been reported to occur up to 17.7%–39% and hemoptysis in 5%–10% of all biopsy procedures (20, 28, 29), our postprocedural complication rates of 17.3% are relatively low. One previous study showed that the use of virtual navigation guidance was able to significantly reduce the occurrence of biopsy-related pneumothorax and hemoptysis (12). We think that our relatively low complication rates could be attributed to the avoidance of emphysema and important vascular structures along the needle trajectory using accurate planning software and navigation systems.

In our study, the total procedure time was 14.6±5.14 min, which was substantially shorter than the reported time of a previous CT-guided localization study (25.6 min) (12). Considering that additional time was spent in our study to determine the trajectories using virtual navigation software, this result is noteworthy. We believe that CBCT and CBCT virtual navigation systems based on 3D CBCT data can enable easier and more precise needle guidance through PTL procedures in a more comfortable and confident manner, which can then lead to shorter total procedure times.

In our study, the mean effective dose of CBCT virtual navigation-guided PTL was 5.21 mSv. This result is similar to that of the previous CBCT-guided PTNB study (5.72 mSv) (11). As with the previous study (11), we performed CBCT approximately three times for each nodule (mean, 3.2±0.7): the initial CT for preprocedural planning, the second for the exact location of the coaxial needle tip around target points, and the third for evaluation of postprocedural complication. These results of radiation exposure are similar, or somewhat lower, compared with those of CTF-guided PTNB (6.53 mSv) (20). We believe that the current radiation dose during CBCT virtual navigation-guided PTL is not a substantial hindrance. However, increased awareness and efforts such as the application of a reasonably small field-of-view or collimation should be used to reduce radiation exposure during PTL.

Although lipiodol-related acute pulmonary embolism has been reported (16), small amounts of lipiodol usage have been reported to be safe for the localization of small pulmonary nodules (30, 31). Kawana-

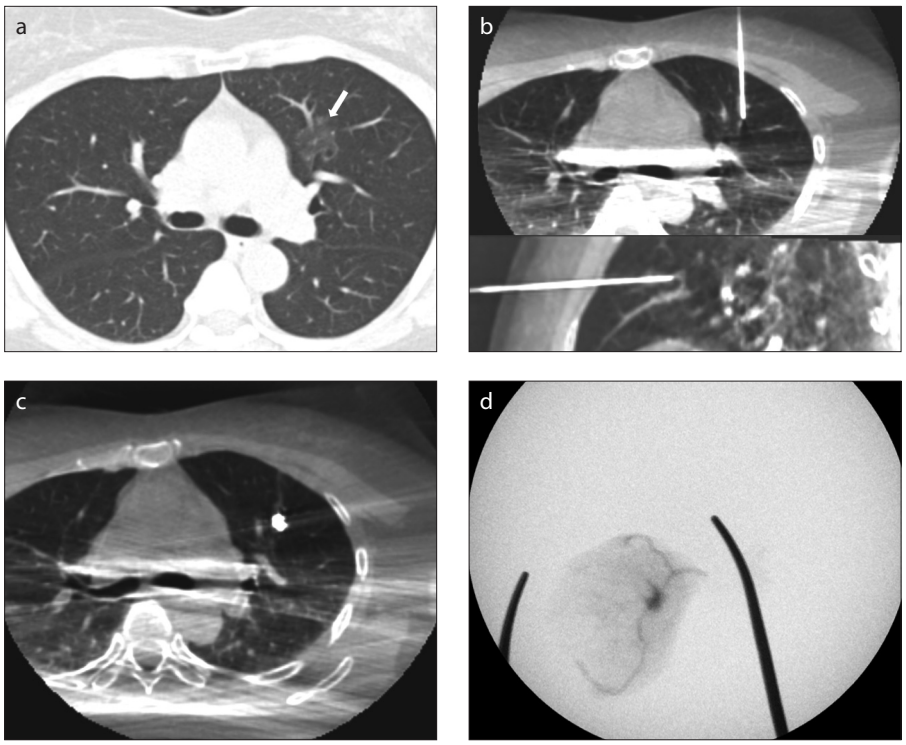

Figures 4. a–d. A 51-year-old female who had CBCT-guided PTL for a 20 mm incidentally-detected pure GGN in the left upper lobe of the lung. This GGN is located very close to subsegmental pulmonary vessels **(a)**. Prior to PTL **(b)**, thorough planning was done to achieve a safe needle trajectory avoiding the abovementioned pulmonary vessels. Needle insertion was performed under CBCT with virtual navigation guidance. Finally, lipiodol was carefully injected through the needle **(c)**, forming a radiopaque marker. There were no procedure-related complications. During the video-assisted thoracoscopic surgery, the localized marker was easily detectable by intraoperative fluoroscopy. The localized marker is also easily detectable by fluoroscopy in the excised specimen **(d)**. This nodule was proven to be a minimally-invasive adenocarcinoma.

ka et al. (8) reported 0.3–0.5 mL of lipiodol marking was safe in their 107 cases without any lipiodol-related complication. In our study, 0.2 mL or less of lipiodol was used and there were no lipiodol-related complications with this minimal usage. However, it should be kept in mind that embolization can be a possible complication of lipiodol use; the placement of the needle tip within the pulmonary vessel and any movement of lipiodol droplets during the lipiodol injection must be monitored carefully.

There are several limitations to our study. First, our study had a retrospective design with a relatively small study population. Second, we did not review the resected surgical specimen containing lipiodol markers, thus we did not evaluate the histopathologic effects of lipiodol on the nodule pathology. However, according to several previous studies, lipiodol is a safe and inert material without adverse effects on the histologic diagnosis due to inflammatory reaction (17, 27, 32–34). In the present study, there were no cases in which a definitive pathologic diagnosis had been hindered due to lipiodol markers. Third, our study was not designed to directly compare CBCT virtual navigation-guided PTL with CBCT-guided PTL without navigation systems or CT- or CTF-guided PTL, thus we could not state definitively which guiding modality would be the best.

In conclusion, PTL can be performed under the guidance of CBCT virtual navigation system in a very accurate and safe manner.

Financial disclosure

This work was supported by the Industrial Strategic technology development program (grant number: 10041618) funded by the Ministry of Trade Industry and Energy (MI).

Conflict of interest disclosure

The authors declared no conflicts of interest.

References

1 Henschke CI, McCauley DI, Yankelevitz DF, et al. Early lung cancer action project: overall design and findings from baseline screening. Lancet 1999; 354:99–105. [CrossRef]
2 Henschke CI, Yankelevitz DF, Mirtcheva R, McGuinness G, McCauley D, Miettinen OS. CT screening for lung cancer: frequency and significance of part-solid and nonsolid nodules. AJR Am J Roentgenol 2002; 178:1053–1057. [CrossRef]
3 Lal H, Neyaz Z, Nath A, Borah S. CT-guided percutaneous biopsy of intrathoracic lesions. Korean J Radiol 2012:13:210–226. [CrossRef]
4 Kim H, Park CM, Koh JM, Lee SM, Goo JM. Pulmonary subsolid nodules: what radiologists need to know about the imaging features and management strategy. Diagn Interv Radiol 2014; 20:47–57.
5 Hirai S, Hamanaka Y, Mitsui N, Morifuji K, Uegami S. Role of video-assisted thoracic surgery for the diagnosis of indeterminate pulmonary nodule. Ann Thorac Cardiovasc Surg 2006; 12:388–392.
6 Chen S, Zhou J, Zhang J, et al. Video-assisted thoracoscopic solitary pulmonary nodule resection after CT-guided hookwire localization: 43 cases report and literature review. Surg Endosc 2010; 25:1723–1729. [CrossRef]
7 Karasaki T, Nakajima J, Murakawa T, et al. Video-assisted thoracic surgery lobectomy preserves more latissimus dorsi muscle than conventional surgery. Interact Cardiovasc Thorac Surg 2008; 8:316–320. [CrossRef]
8 Kawanaka K, Nomori H, Mori T, et al. Marking of small pulmonary nodules before thoracoscopic resection. Acad Radiol 2009; 16:39–45. [CrossRef]
9 Zaman M, Bilal H, Woo CY, Tang A. In patients undergoing video-assisted thoracoscopic surgery excision, what is the best way to locate a subcentimetre solitary pulmonary nodule in order to achieve successful excision? Interact Cardiovasc Thorac Surg 2012; 15:266–272. [CrossRef]
10 Lee NK, Park CM, Kang CH, et al. CT-guided percutaneous transthoracic localization of pulmonary nodules prior to video-assisted thoracoscopic surgery using barium suspension. Korean J Radiol 2012; 13:694–701. [CrossRef]
11 Choo JY, Park CM, Lee NK, Lee SM, Lee HJ, Goo JM. Percutaneous transthoracic needle biopsy of small (≤1 cm) lung nodules under C-arm cone-beam CT virtual navigation guidance. Eur Radiol 2012; 23:712–719. [CrossRef]
12 Lee SM, Park CM, Lee KH, Bahn YE, Kim JI, Goo JM. C-arm cone-beam CT-guided percutaneous transthoracic needle biopsy of lung nodules: clinical experience in 1108 patients. Radiology 2014; 271:291–300. [CrossRef]
13 Jin KN, Park CM, Goo JM, et al. Initial experience of percutaneous transthoracic needle biopsy of lung nodules using C-arm cone-beam CT systems. Eur Radiol 2010; 20:2108–2115. [CrossRef]
14 Choi JW, Park CM, Goo JM, et al. C-Arm cone-beam CT–guided percutaneous transthoracic needle biopsy of small (≤ 20 mm) lung nodules: diagnostic accuracy and complications in 161 patients. AJR Am J Roentgenol 2012; 199:W322–W330. [CrossRef]
15 Wallace MJ, Kuo MD, Glaiberman C, Binkert CA, Orth RC, Soulez G. Three-dimensional C-arm cone-beam CT: applications in the interventional suite. J Vasc Interv Radiol 2008; 19:799–813. [CrossRef]
16 Papiamonis NE, Matrella E, Blevrakis EG, Kouroumalis EA. Acute pulmonary embolism following N-butyl-cyanoacrylate endoscopic injection sclerotherapy. Ann Gastroenterol 2012; 25:261.

17 Watanabe K, Nomori H, Ohtsuka T, Kaji M, Naruke T, Suemasu K. Usefulness and complications of computed tomography-guided lipiodol marking for fluoroscopy-assisted thoracoscopic resection of small pulmonary nodules: experience with 174 nodules. J Thorac Cardiovasc Surg 2006; 132:320–324. [CrossRef]
18 Finley RJ, Mayo JR, Grant K, et al. Preoperative computed tomography–guided microcoil localization of small peripheral pulmonary nodules: a prospective randomized controlled trial. J Thorac Cardiovasc Surg 2015; 149:26–32. [CrossRef]
19 Heck SL, Blom P, Berstad A. Accuracy and complications in computed tomography fluoroscopy-guided needle biopsies of lung masses. Eur Radiol 2006; 16:1387–1392. [CrossRef]
20 Kim GR, Hur J, Lee SM, et al. CT fluoroscopy-guided lung biopsy versus conventional CT-guided lung biopsy: a prospective controlled study to assess radiation doses and diagnostic performance. Eur Radiol 2011; 21:232–239. [CrossRef]
21 Paulson EK, Sheafor DH, Enterline DS, McAdams HP, Yoshizumi TT. CT fluoroscopy-guided interventional procedures: techniques and radiation dose to radiologists. Radiology 2001; 220:161–167. [CrossRef]
22 Silverman SG, Tuncali K, Adams DF, Nawfel RD, Zou KH, Judy PF. CT fluoroscopy-guided abdominal interventions: techniques, results, and radiation exposure. Radiology 1999; 212:673–681. [CrossRef]
23 Nawfel RD, Judy PF, Silverman SG, Hooton S, Tuncali L, Adams DF. Patient and personel exposure during CT Fluoroscopy-guided interventional procedures. Radiology 2000; 216:180–184. [CrossRef]
24 Cazzato RL, Battistuzzi JB, Catena V, et al. Cone-beam computed tomography (CBCT) versus CT in lung ablation procedure: which is faster? Cardiovasc Intervent Radiol 2015; 38:1231–1236. [CrossRef]
25 Cazzato RL, Buy X, Alberti N, Fonck M, Grasso RF, Palussière J. Flat-pane cone-beam CT-guided radiofrequency ablation of very small (≤ 1.5cm) liver tumors: technical note on a preliminary experience. Cardiovasc Intervent Radiol 2015; 38:206–212. [CrossRef]
26 Rafiei P, Kim SK, Kamran M, Saad NE. Retrospective study in 40 patients of utility of C-arm FDCT as an adjunctive modality in technically challenging image-guided percutaneous drainage procedures. Cardiovasc Intervent Radiol 2015; 38:1589–1594. [CrossRef]
27 Hwang HS, Chung MJ, Lee JW, Shin SW, Lee KS. C-arm cone-beam CT-guided percutaneous transthoracic lung biopsy: usefulness in evaluation of small pulmonary nodules. AJR Am J Roentgenol 2010; 195:W400–407. [CrossRef]
28 Priola AM, Priola SM, Cataldi A, et al. Diagnostic accuracy and complication rate of CT-guided fine needle aspiration biopsy of lung lesions: a study based on the experience of the cytopathologist. Acta Radiol 2010; 51:527–533. [CrossRef]
29 Ko JP, Shepard JO, Drucker EA, et al. Factors influencing pneumothorax rate at lung biopsy: Are dwell time and angle of pleural puncture contributing factors? Radiology 2001; 218:491–496. [CrossRef]
30 Jin KN, Lee KW, Kim TJ, Song YS, Kim DI. Computed tomography guided percutaneous injection of a mixture of lipiodol and methylene blue in rabbit lungs: evaluation of localization ability for video-assisted thoracoscopic surgery. J Korean Med Sci 2014; 29:129–136. [CrossRef]
31 Kim YD, Jeong YJ, I H, et al. Localization of pulmonary nodules with lipiodol prior to thoracoscopic surgery. Acta Radiol 2011; 52:64–69. [CrossRef]
32 Nomori H, Horio H, Naruke T, Suemasu K. Fluoroscopy-assisted thracoscopic resection of lung nodules marked with lipiodol. Ann Thorac Surg 2002; 74:170–173. [CrossRef]
33 Kang DY, Kim HK, Kim YK, Yong HS, Kang EY, Choi YH. Needlescopy-assisted resection of pulmonary nodule after dual localisation. Eur Respir J 2010; 37:13–17. [CrossRef]
34 Yamagami T, Miura H, Yoshimatsu R, et al. Experience of fluoroscopy-aided thoracoscopic resection of pulmonary nodule localised with Lipiodol in a child. J Med Imaging Radiat Oncol 2011; 55:401–403.[CrossRef]